Desalination and Water Treatment
www.deswater.com

doi: 10.5004/dwt.2021.27034

221 (2021) 163–175
May

Chemically modified rhamnogalacturonans from linseed: a supersorbent for Cd^{2+} and Pb^{2+} uptake from aqueous solution

Muhammmad Ajaz Hussain[a,*], Summia Gul[a], Azhar Abbas[a], Arshad Ali[a], Nasser Fahad Alotaibi[b]

[a]*Institute of Chemistry, University of Sargodha, Sargodha 40100, Pakistan, emails: majaz172@yahoo.com (M.A. Hussain), azharabbas73@yahoo.com (A. Abbas), arshadali04@yahoo.com (A. Ali)*
[b]*Chemistry Department, College of Science, Jouf University, Aljouf, Sakaka, Saudi Arabia, email: nfalotaibi@ju.edu.sa*

Received 2 September 2020; Accepted 31 December 2020

ABSTRACT

Herein, this study rhamnogalacturonans (RG) was isolated from linseed and chemically modified to its succinate (SRG) by reacting it with succinic anhydride. Then, SRG was converted into the sodic form using $NaHCO_3$ (Na-SRG). The novel Na-SRG appeared a supersorbent hence it was utilized for the uptake of Cd^{2+} and Pb^{2+} from an aqueous solution. Chemical modification in the structures of the materials was easily characterized by Fourier-transformed infrared (FTIR) spectroscopy and sorbent surface charge was analyzed through zero-point charge (pH_{ZPC}) analyses. Batch series of sorption experimentation were conducted to investigate the influence of initial concentration of Cd^{2+} and Pb^{2+}, sorbent dosage, pH, contact time, and temperature on the sorption capacity of Na-SRG. Maximum sorption capacities (Q_{max} in mg g^{-1}) of sorbent Na-SRG as-evaluated from Langmuir isotherm were found to be 303.03 and 316.79 mg g^{-1} for Cd^{2+} and Pb^{2+}, respectively. The kinetics of sorption of the tested metals follows pseudo-second-order kinetics and reached within 30 min. Negative values of thermodynamic parameters ($\Delta G°$, $\Delta S°$, and $\Delta H°$) were found, which indicated the feasibility and exothermic nature of the sorption process. Additionally, the regeneration studies of tested sorbent were also performed over five successive cycles and an insignificant decrease in sorption capacity was come across which showed that sorbent is regenerable.

Keywords: Esterification; Linseed hydrogel; Pseudo-second-order kinetics; Regeneration; Rhamnogalacturonans

1. Introduction

Being persistent, bioaccumulative, and toxic, heavy metals are inevitable environmental pollutants. Their accumulation into the environment can damage the global stability and causes a potential threat to the health of their consumers including human [1]. The most relevant environmental heavy metals are cadmium (Cd^{2+}) and lead (Pb^{2+}). Both of these metals have many advantageous applications as cadmium is the most widely used metal in industries for the manufacturing of Ni–Cd batteries, in the preparation of cadmium pigments, toys, jewelry items, and in the plastic industry [2–4], while lead is the main precursor of lead-acid storage batteries [5].

Besides their versatile applications, these heavy metals are toxins in the environment and are ubiquitous in different forms. According to World Health Organization (WHO) and US-Environmental Protection Agency (EPA), the threshold level of Cd^{2+} in drinking water is 0.003 mg L^{-1} and Pb^{2+} is 0.05 mg L^{-1}. However, the co-exposure of these heavy metals through natural sources and human activities increasing their concentration from permissible level and causes many disorders in vital body organs [6–8]. Cd^{2+} is carcinogenic and it also induced apoptosis, necrosis, and

---

[*] Corresponding author.

mitochondrial dysfunction [9–11], while the exposure of Pb^{2+} damages the kidney and liver [12,13]. Hence, in order to save life, it is imperative to remove these metals from contaminated water.

Many physico-chemical treatment techniques have been applied previously to remove these metals from unhygienic waters, that is, chemical precipitation [14] reverse osmosis [15], ultrafiltration membranes [16], electro-chemical treatment [17], adsorption [18], etc. Owing to the high enrichment efficiency, ease of phase separation, and use of environmentally friendly and low-cost sorbent, adsorption technology followed by ion-exchange is considered to be one of the promising scientific tools for the removal of heavy metal ions from water bodies nowadays [19]. The use of biological and commercial materials, agro-waste, and activated carbon, are amongst the most popular low-cost biosorbents. But all of these are vulnerable due to their low sorption capacities. Therefore, for this reason, there is a growing interest in developing more economic and eco-friendly sorbent for fine tuning of the polluted water. Polysaccharide-based hydrogels can be modified using anhydrides of carboxylic acid (i.e., succinic anhydride) and deserve special attention to use them as-sorbent for Cd^{2+} and Pb^{2+} removal from wastewater [20,21]. Rhamnogalacturonans-rich mucilages are stimuli-responsive, superporous, superabsorbent, and non-toxic in nature, and have been successfully utilized to develop targeted and sustained release drug delivery system. For example, hydrogel extruded from linseeds/flax seeds (*Linum usitatissimum* L.) as a mucilage, linseed hydrogel (LSH = RG) was used as sustained release material to prepared pH-responsive tablet formulations of diclofinac sodium, caffeine, and diacerein. Moreover, RG has also been used for the development of novel gastroretentive matrix tablets for sustaining the release of antibiotic moxifloxacine [22–24].

In this study, we introduce a supersorbent based on rhamnogalacturonans for Cd^{2+} and Pb^{2+} uptake after its modification. The aims are to modify RG to sodium salt of its succinate derivative (Na-SRG). The sorbent surface charge will be evaluated by analyzing zero-point charge pH, that is, pH_{ZPC}. Also, we are evaluating the effect of different operational parameters such as the initial concentration of Cd^{2+} and Pb^{2+}, sorbent dosage, pH, time of contact, and temperature on sorption capacities. The experimental sorption data will be fitted to different isothermal and kinetic models to explore the possible mechanism involved in this sorption. Moreover, different thermodynamic parameter, that is, a change in free energy ($\Delta G°$), enthalpy ($\Delta H°$), and change in entropy ($\Delta S°$) has been examined to assess the feasibility and nature of sorption. We also investigated the reproducibility studies of this novel bio-based supersorbent.

2. Materials and methods

2.1. Materials

The *L. usitatissimum* seeds (linseeds/flax seed) were purchased from the local market and used to get linseed hydrogel (LSH = RG). The seeds were manually cleaned and sieved from filthy materials. Deionized water (DW) was used to perform the entire experimental work. Solvents and reagents, that is, Succinic anhydride (100.07 g mol^{-1}, 99%) *N,N*-dimethylacetamide (87.12 g mol^{-1}, 99%), 4-dimethylaminopyridine (122.17 g mol^{-1}, 99%), HCl (36.46 g mol^{-1}, 99%), NaOH (39.997 g mol^{-1}, 99%), sodium bicarbonate (80.007 g mol^{-1}, 99%), sodium nitrate (84.9947 g mol^{-1}, 99%) (Alfa Aesar, Kandel Germany), acetone (58.08 g mol^{-1}, 99%), *n*-hexane (86.18 g mol^{-1}, 99%) (Riedel-de-Haen, Germany), $NaNO_3$ (84.9947 g mol^{-1}, 99%), $AgNO_3$ (169.87 g mol^{-1}, 99%), $Pb(NO_3)_2$ (331.00 g mol^{-1}, 99%), and $CdCl_2$ (183.32 g mol^{-1}, 99%) (Sigma-Aldrich, USA) used in the experimental work were of analytical grade and used as such without further purification. All glassware were washed and rinsed with nitric acid (HNO_3, 63.01 g mol^{-1}, 99%) prior to use in the experimental work.

2.2. Isolation of hydrogel from linseed

The RG was isolated as per method given by Haseeb et al. [22] with little/necessary modification. Briefly, linseeds were allowed to swell in DW for 48 h at room temperature (RT) and then warmed at 80°C for 1 h. The mucilage extruded from seeds was detached using nylon mesh followed by rubbing with spatula and purified/de-fatted by washing with *n*-hexane (three times) and then with the DW. The obtained mucilage, i.e., Linseed hydrogel (RG) was isolated in a pellet form after centrifugation at 4,000 rpm for 2 h. RG was spread on a steel tray and kept in a vacuum oven at 50°C. Ultimately, dried RG was ground to a fine powder after sieving through mesh sieve no. 60 and stored in an air-tight jar in a desiccator under vacuum.

2.3. Synthesis of SRG and sorbent Na-SRG

Pre-dried RG (3.0 g) was added in *N,N*-dimethylacetamide (DMAc) (40 mL) to prepare its suspension by heating at 80°C for 1 h under continuous stirring at 200 rpm. To the homogenized suspension of RG in DMAc, succinic anhydride (11.10 g) was added along with catalytic amount of 4-dimethylaminopyridine (DMAP) (0.05 g) and the reaction was kept under constant stirring at 70°C for 24 h. The reaction mixture was then cooled at RT and washed in 100 mL acetone thrice to make it free from succinic acid and unreacted succinic anhydride. The resultant succinate of rhamnogalacturonans (SRG) was dried in a vacuum oven at 50°C and then ground to powdered form.

For the synthesis of sodic form of SRG (Na-SRG), SRG was stirred in a saturated solution of $NaHCO_3$ in DW for 2 h at RT. The as-forming suspension was filtered to obtained Na-SRG and washed with DW several times (until the neutralization of filtrate) to remove the traces of $NaHCO_3$. The Na-SRG was then dried in an oven under vacuum at 50°C and stored in air-tight jar to use it as sorbent for the removal of Cd^{2+} and Pb^{2+} from an aqueous solution.

2.4. Determination of DS

The DS value of the newly synthesized SRG was determined using a standard acid-base titration method [25]. For this purpose, 0.1 g of SRG was stirred in 100 mL of 0.02 M $NaHCO_3$ at room RT for 2 h. The solution was filtered and a known volume of $NaHCO_3$ solution was taken to titrate it against 0.02 M solution of HCl using phenolphthalein indicator. The net volume of HCl used for titration against $NaHCO_3$ was feed in Eq. (1) to calculate the DS value of SRG using Eq. (2):

$$n_{\text{suc}} = V_{\text{NaHCO}_3} \times M_{\text{NaHCO}_3} - V_{\text{HCl}} \times M_{\text{HCl}} \tag{1}$$

$$\text{DS} = \frac{162.14 \times n_{\text{suc}}}{m_{\text{SRG}} - 100 \times n_{\text{suc}}} \tag{2}$$

where, V_{NaHCO_3}, M_{NaHCO_3}, V_{HCl}, M_{HCl}, n_{suc}, and m_{SRG} represents the volume of $NaHCO_3$, the molarity of $NaHCO_3$, the volume of HCl, the molarity of HCl, number of moles of free carboxylic acid moieties, and the mass of SRG in g, respectively. whereas 162.14 g mol^{-1} is taken as the molar mass of an anhydrous glucose unit (AGU) assumed for each substituted succinyl moiety and 100 g mol^{-1} is the net increase in the mass of an AGU.

2.5. Calculation of the yield of SRG

Pre-calculated DS value of SRG was put in Eq. (3) to calculate the theoretical yield of the esterification reaction between RG and SAn:

$$\text{Theoretical yield} = m_{\text{RG}} + \left[\frac{m_{\text{SRG}}}{M_{\text{SRG}}} \times \text{DS} \times M_{\text{suc}} \right] \tag{3}$$

where m_{RG} is the mass of repeating unit of RG, m_{SRG} is the mass of SRG, M_{SRG} is the molar mass of SRG and M_{suc} is the molecular mass of succinic acid.

2.6. Characterization

The IR Prestige-21 spectrophotometer (Shimadzu, Japan) was used to record the FTIR (KBr) spectrum of the RG, SRG, and Na-SRG. A flame atomic absorption spectrophotometer (FAAS, AA 6300 Shimadzu, Japan) equipped with air–acetylene flame was used to estimate the residual concentrations of and Cd^{2+} and Pb^{2+}in the given sample. The Cd^{2+} and Pb^{2+} atoms in a gaseous state were irradiated with optical radiation of fixed wavelength, that is, 228.8 nm for Cd^{2+} and 283.3 nm for Pb^{2+}. The radiation flux was measured using the detectors of respective metals and analyte concentration was determined using Beer–Lambert law. Zero-point charge pH (pH_{ZPC}) of sorbent Na-SRG was determined by the pH-drift titration.

2.7. Sorption studies

A series of equilibrium sorption experimentation was carried out to optimize the ideal conditions at which sorbent Na-SRG can uptake maximum amount of Cd^{2+} and Pb^{2+} from aqueous solution, and to explore the dependence of various operational parameters, like initial Cd^{2+} and Pb^{2+} concentration, sorbent dosage, pH, contact time, and temperature on the sorption capacity of sorbent. To investigate these effects (1,000 mg L^{-1}, 1,000 mL) stock solution was prepared by dissolving 1.63 g of $CdCl_2$ and 1.60 g of $Pb(NO_3)_2$ in DW. The prepared stock solutions of both metals were diluted to a required concentration in each parameter and the pH of working solutions was adjusted to the required value using 0.1 M HCl or 0.1 M NaOH. Metal ion solutions of known concentration (100 mg L^{-1}, 100 mL) were taken in Erlenmeyer flasks and shaken using a shaking thermostat machine for 30 min at a fixed temperature. Soon thereafter, sorbent was separated from the solution by filtration and remaining concentrations of Cd^{2+} and Pb^{2+} in the supernatant layer was determined using FAAS at 228.8 nm and 283.3 wavelengths, respectively for Cd^{2+} and Pb^{2+}. Amounts of Cd^{2+} and Pb^{2+} sorbed by Na-SRG, that is, q_e (mg g^{-1}) and the % age uptake capacity was calculated by equations below:

$$q_e = \frac{C_i - C_e}{m} \times V \tag{4}$$

$$\text{Percentage uptake} = \frac{C_i - C_e}{C_i} \times 100 \tag{5}$$

where the parameter q_e is the equilibrium sorption capacity of Na-SRG in mg g^{-1}, C_i is the initial metal concentration in mg L^{-1}, C_e is the residual concentration in mg L^{-1}, V represents the volume of the solution used for sorption studies (L), and m is the mass of sorbent used (g).

2.7.1. Effect of initial metal ion concentration

The dependence of the sorption process of Cd^{2+} and Pb^{2+} sorption on initial metal ion concentrations was studied by agitating 30 mg sorbent with 100 mL metal ion solution of different concentrations (20, 40, 60, 80, 100, 120, 140, and 160 mg L^{-1}) for both Cd^{2+} and Pb^{2+} for 30 min at a speed of 200 rpm and 298 K temperature. From the study of the effect of initial metal ion concentration, sorption equilibrium was established by feeding experimental sorption data to Freundlich and Langmuir isothermal models and initial metal ion concentration was optimized for further sorption experimentations.

2.7.2. Effect of sorbent dose

To evaluate the minimum amount of sorbent at which it can adsorbed maximum amount of Cd^{2+} and Pb^{2+} from aqueous solution, different sorbent quantities ranging from 20 to 90 mg/100 mL of Na-SRG was added to 100 mg L^{-1} solutions of Cd^{2+} and Pb^{2+}. Here, sorbent dosage was optimized.

2.7.3. Effect of pH

To select the pH at which maximum sorption can occur, the effect of pH on the sorption capacity of the sorbent under study was evaluated by adding pre-optimized amount of sorbent (30 mg) into 100 mg L^{-1} solutions (100 mL) of both the tested metals. The pH of solutions containing Cd^{2+} and Pb^{2+} was varied from 2 to 10 and adjusted using 1 M solution of HNO_3 and 1 M NaOH.

2.7.4. Effect of contact time

The effect of contact time was compiled to study the sorption kinetics (i.e., pseudo-first-order and pseudo-second-order) and to know about the mechanism of sorption. For this purpose, an optimum amount of sorbent (30 mg), at optimum initial metal ion concentration (100 mg L^{-1} for Cd^{2+} and Pb^{2+}) and pH = 6, was dissolved in Cd^{2+} and Pb^{2+} ions containing solutions (100 mL) at RT (298 K) for different time intervals, that is, for 5–120 min. The equilibrium concentration of metal ions was measured by FAAS.

2.7.5. Effect of temperature

The nature of sorption process (exothermic/endothermic and spontaneous/non-spontaneous) was intimated by knowing the effect of temperature on sorption. To do so, similar procedure, as used for the study of other sorption experiments, was adopted in the range of temperature from 298 to 348 K.

2.7.6. Sorption and desorption (regenerability)

Regeneration studies were also carried out for this sorbent. For this purpose, the sorbent was first stirred with metal ion solutions for 30 min. This stirring converted Na-SRG into Cd-SRG and Pb-SRG. Then the solution was filtered off and the recovered sorbent (which was now Cd-SRG and Pb-SRG) was treated with brine (saturated aqueous solution of NaCl) for desorption of Cd^{2+} and Pb^{2+} ions. The Cd^{2+} and Pb^{2+} ions were replaced with Na^+ and Na-SRG was regenerated. This process was repeated for five times and after each regeneration phase, the sorbent was centrifuged, air-dried, and washed with DW extensively before the next cycle until it gives a negative test with silver nitrate ($AgNO_3$).

2.8. Determination of thermodynamic parameters

To determine whether the sorption process is feasible or not-feasible, spontaneous or non-spontaneous, and exothermic or endothermic, experimental data obtained from the effect of temperature studied for sorption of Cd^{2+} and Pb^{2+} by sorbent Na-SRG was used to value different thermodynamic parameters, such as a change in free energy ($\Delta G°$), enthalpy ($\Delta H°$), and entropy ($\Delta S°$) using the following equations:

$$K_C = \frac{C_{\text{ads}}}{C_e} \tag{6}$$

$$\ln K_C = \frac{\Delta S°}{R} - \frac{\Delta H°}{RT} \tag{7}$$

$$\Delta G° = -RT\ln K_C \tag{8}$$

In these equations, C_{ads} is the adsorbed metal and C_e is the concentration of metal ions at equilibrium. K_C is the sorption equilibrium constant. R (8.314 $JK^{-1}Mol^{-1}$) is the general gas constant. Plot of a graph $\ln K_C$ and $1/T$ (K^{-1}) helps for required calculations using slope and intercept of graph.

The aforesaid sorption experiments were conducted in triplicate and the average of values was used to record the results.

3. Results and discussions

3.1. Synthesis of SRG and sorbent Na-SRG

Esterification strategy was used to chemically modify the RG. Amongst the ester derivatives of naturally occurring polysaccharides materials in seed mucilage, succinate derivatives are reportedly the best choice for heavy metal ion uptake from solutions and high-hardness groundwater [26–28]. To carry out this conversion, Linseed mucilage (RG) was treated with succinic anhydride in the presence of solvent DMAc. Following is the FTIR and DS data.

Yield: 2.13 g; degree of substitution (DS): 1.60/anhydroglucose repeating unit

FTIR (KBr); 3,356 (OH); 2,936 (CH and CH_2); 1,726 ($C = O_{\text{ester}}$); and 1,028 (C–O–C) cm^{-1}

The resulted succinylated product, that is, SRG was then modified to its sodium salt (Na-SRG) by tuning with saturated aqueous solution of $NaHCO_3$ (100 mL). Following is the FTIR and DS data.

FTIR (KBr); 3,603 (OH); 2,902 (CH and CH_2); 1,730 ($C = O_{\text{ester}}$); 1,570 (COO^-); and 1,039 (C–O–C) cm^{-1}

The Na-SRG is considered to serve as an ideal material (supersorbent) for the uptake of Cd^{2+} and Pb^{2+} from aqueous solution because it has exchangeable Na^+ ions which can enhance its ability to uptake metal ions.

Homogeneous-reaction conditions as described by Abbas et al. [29] were maintained to achieve aforesaid conversion chain. The reaction yield was found to be 2.13 g on account of succinate moieties with 1.6 DS value of succinyl functionalities per AGUs. The schematic synthesis of SRG and Na-SRG is depicted in Fig. 1.

3.2. FTIR spectroscopic analysis

Fig. 2 shows the FTIR (KBr) spectra of hydrogel sample (RG), and products (SRG and Na-SRG). The appearance of a prominent peak of carbonyl moiety at 1,726 cm^{-1} in the spectrum of SRG (Fig. 2b) confirms the success of esterification reaction between RG and succinic anhydride, that is, formation of SRG. This peak shifts to a longer wavenumber 1,730 cm^{-1} in the spectrum of Na-SRG. Additionally, the appearance of a peak at 1,570 cm^{-1} is due to the presence of carboxylate anion ($–COO^-$) of the Na-SRG [30]. Beside these absorption signals, all other basic signals signifying the polymeric backbone also appeared at 3,603 (O–H); 2,902 (C–H); and 1,039 (C–O–C) cm^{-1} in the spectra of Na-SRG (Fig. 2c).

3.3. Determination of zero-point charge pH (pH_{ZPC})

The zero-point charge pH (pH_{ZPC}) in the phenomenon of sorption describes the point at which there is zero electrical charge on the surface of sorbent. At pH_{ZPC}, the surface of sorbent endures no charge due to the equality of total charge of all positively charged surfaces and total charge of all negatively charged surfaces [31]. At pH greater than pH_{ZPC}, the surface of sorbent is negatively charged and it can interact with positively charged metal ions, whereas at pH lower than pH_{ZPC}, sorbent surface is positively charged and can interact with negatively charged species. So, to predict the suitability of sorbent for sorption study, it is of utmost important to know its pH_{ZPC}. The pH_{ZPC} of sorbent Na-SRG

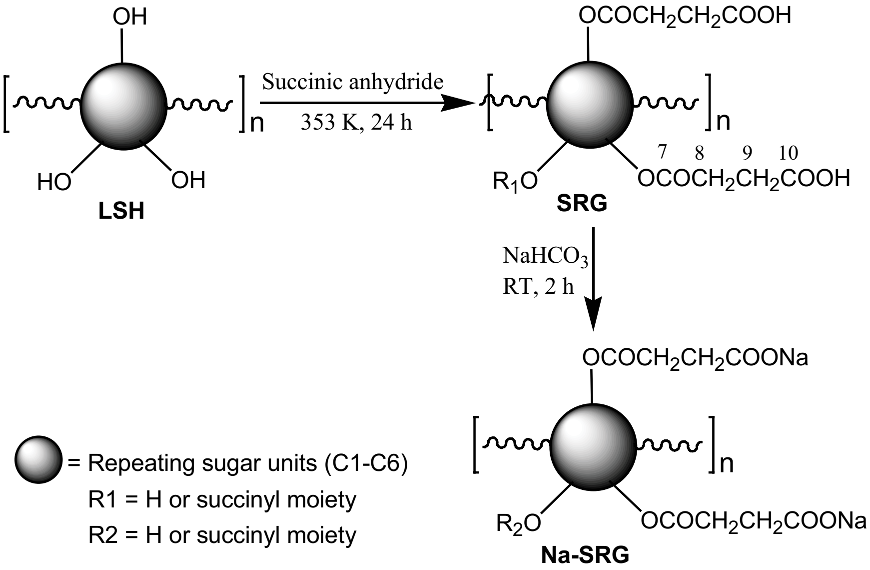

Fig. 1. Scheme for the synthesis of SRG and Na-SRG.

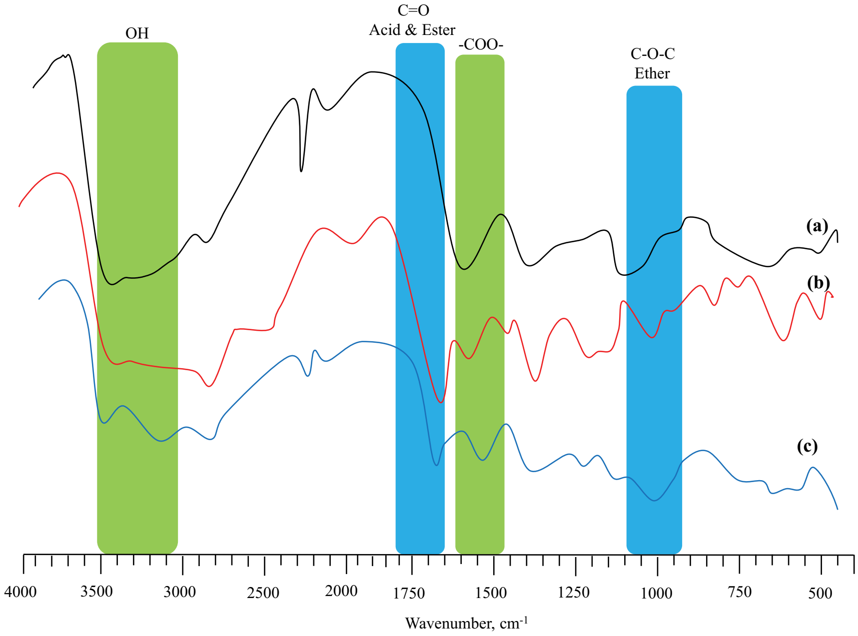

Fig. 2. Overlay FTIR (KBr) spectra of RG (a), SRG (b), and Na-SRG (c).

was determined using pH-drift titration as described by Jiao et al. [32]. For this purpose, 50 mg of Na-SRG was dissolved in 100 mL of DW in separate beakers. The pH_i (initial pH) of corresponding solutions was adjusted from 1 to 7 using 0.1 M solution of HCl/NaOH and solutions were then subjected under shaking for 2 h at 200 rpm at RT. The pH_f (final pH) values were calculated for the supernatant liquid and the difference between pH_i and pH_f ($pH_i - pH_f$) was taken and plotted against pH_i. The pH_{ZPC} of the sorbent Na-SRG was found to be 4.7 (Fig. 3) which indicated the presence of weak carboxylic acid (–COOH) functionality having weak acidic character. The surface of the sorbent Na-SRG becomes negatively charged at pH greater than 4.7 which favors the uptake of Cd^{2+} and Pb^{2+} ions.

3.4. Sorption studies

3.4.1. Effect of initial metal ion concentration

The effect of initial metal ion concentration on the activity of sorbent was explored. Fig. 4a elucidates the effect of initial Cd^{2+} and Pb^{2+} concentration on sorption capacity which shows that the sorption capacity of the sorbent Na-SRG increases as the concentration of metal ions

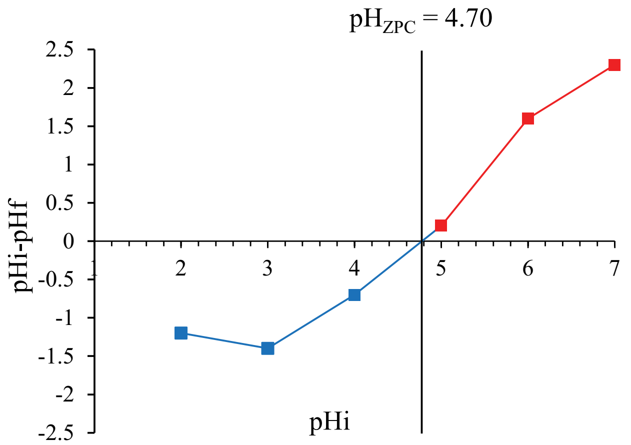

Fig. 3. Zero-point charge pH (pH_{ZPC}) analysis of Na-SRG sorbent.

increases and later after achieving saturation it becomes constant. The sorption capacity (q_e in mg g^{-1}) reached to the highest value at 100 mg L^{-1} for both Cd^{2+} and Pb^{2+}. The main reason behind this trend is that as the concentration of metal ions was increased in their corresponding solutions the availability of Cd^{2+} and Pb^{2+} ions for sorbent Na-SRG also increases. However, after achieving saturation (after 100 mg L^{-1}), the surface-active sites on the Na-SRG consumed due to which all the exchangeable ions (Na^+) of sorbent might exchange with ions of sorbate (Cd^{2+} and Pb^{2+}). Consequently, the sorption capacity becomes perpetual [33].

3.4.2. Effect of sorbent dosage

The minimum amount of sorbent at which maximum sorption capacity can achieve was also optimized. It was observed that by increasing sorbent dosage, there were more and more uptakes of Cd^{2+} and Pb^{2+} from the aqueous solution because with the increase in sorbent dosage the number of active sites for the sorption also increases. There was a significant decrease in the uptake of these metal ions after the optimum level (30 mg). This can be explained by the fact that no more ions were available to be sorbed by the sorbent after the optimum level [28]. Therefore, 30 mg was found to be the optimum dosage of sorbent to uptake Cd^{2+} and Pb^{2+} and used for further experimental work (Fig. 4b).

3.4.3. Effect of pH

The alteration in pH of the solution may change the sorbent surface charge and its ability to ionize. Therefore, it is of utmost important to investigate the influence of pH on the sorption capacity of sorbent Na-SRG. The pH range selected for this purpose was 2.0–10.0 for both of the tested metals. Results depicted in Fig. 4c show that at lower pH, sorption of Cd^{2+} and Pb^{2+} is negligible. This low sorption capacity is attributed to the fact that at lower pH due to acidic environment, the sorbent Na-SRG gets protonation and results in the formation of SRG (acidic form of sorbent). As SRG has no metallic ion-exchange affinity, so offers insignificant sorption. Moreover, the graph reveals that with increase in pH value, the uptake of Cd^{2+} and Pb^{2+} also increased. Maximum sorption was noted at pH 6.0 for the tested metals, that is, Cd^{2+} and Pb^{2+}. This might be due to the reason that, once the pH of solution containing Cd^{2+} and Pb^{2+} becomes greater than $pH_{ZPC,}$ then functional groups might de-protonated which in return furnish negative charge at the surface of Na-SRG and favor for sorption. Contrary, at pH_{ZPC}, due to protonation of Na-SRG, its surface became positively charged or either it may get precipitated or partially hydrolyzed to $Cd(OH)_2$ and $Pb(OH)_2$ [34–37]. Consequently, the concentration of Cd^{2+} and Pb^{2+} in the solution decreased and the efficiency of sorbent to sorbed them was stifled. Hence, did not favor for sorption. Therefore, pH = 6 was taken as an optimum pH to carry out all other sorption experiments.

3.4.4. Effect of contact time

Time of contact between exchangeable sites of sorbent and sorbate also affect the sorption capacity of a particular sorbent. If we know the effect of contact time on the sorption capacity of sorbent, then not only we can better establish the mechanism for the uptake of heavy metal ions by prepared sorbent but also we can build kinetic models. For the sake of this connection, effect of time on sorption capacity of Na-SRG was studied. The result reveals that almost 85% of Cd^{2+} and Pb^{2+} were sorbed within first 30 min (optimum time) from an aqueous solution containing both of these metals (Fig. 4d). This might be because at the beginning, the rate of exchange of Cd^{2+} and Pb^{2+} ions of sorbate with Na^+ ions of sorbent was highest due to the presence of a larger number of sodium-succinate moieties on the surface of Na-SRG. Graph also indicated that as the time of contact increase, the repulsive forces between Cd^{2+} and Pb^{2+} and aqueous media will become prominent and impeded the active sites of sorbent. Hence, sorbent will befit to sorb more and more Cd^{2+} and Pb^{2+}. So, no more considerable increase in sorption capacity was found beyond 30 min [30].

3.4.5. Effect of temperature

By knowing the effect of temperature on metal sorption capacities of Na-SRG, the thermodynamic behavior of sorbent via exothermic or endothermic can be explained. For this purpose, the sorption process was monitored at different temperatures ranging from 298 to 343 K. Fig. 4e reveals that at low temperature, the sorption capacity is high but with an increase in temperature sorption capacity decrease.

This is due to the reason that at low temperature the ions (Na^+) are less mobile and there is a greater chance of the Cd^{2+} and Pb^{2+} to get adsorbed on the surface of Na-SRG. While at high temperature the ions (Na^+) are more mobile which offer negligible interaction and leads to decrease in sorption capacity. The said quarries inferred that at 298 K (optimized) sorbent Na-SRG can sorbed the maximum amount of Cd^{2+} and Pb^{2+} from their corresponding solutions.

3.5. Isothermal modeling

Sorption isotherms can be used to explain the equilibrium relationship between the concentration of sorbate in solution and its sorbed concentration under stated conditions.

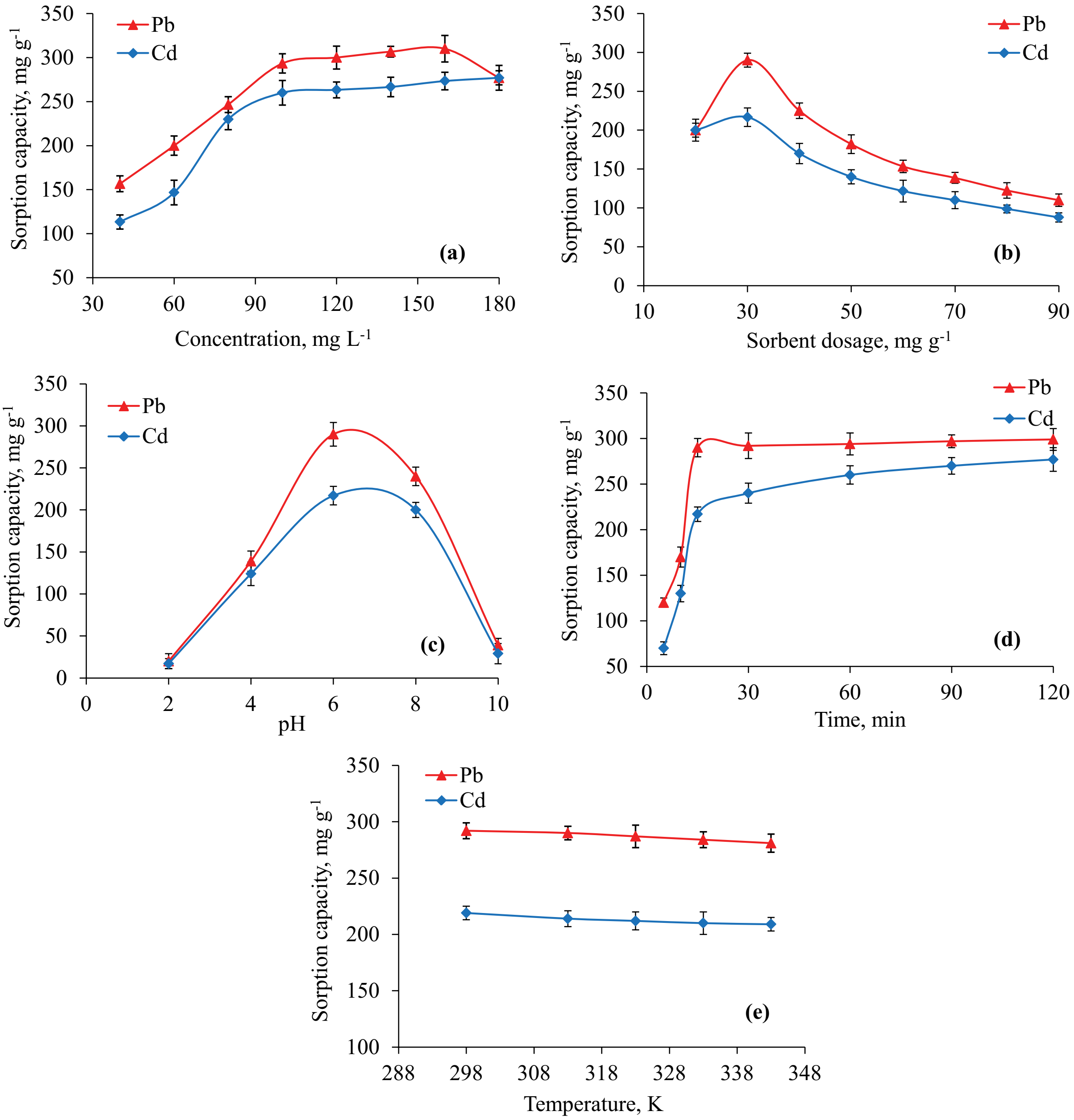

Fig. 4. Effect of initial concentration (a), sorbent dosage (b), pH (c), time (d), and temperature (e) on sorption capacity of Na-SRG for removal of Cd^{2+} and Pb^{2+} ions.

The experimental sorption data acquired from the effect of initial Cd^{2+} and Pb^{2+} concentration on the sorption capacity of Na-SRG to sorbed Cd^{2+} and Pb^{2+} from their respective solutions were used to study this equilibrium relationship and to developed Freundlich and Langmuir isotherms. Additionally, these models could also be used to explain the nature of the mechanism of sorption phenomena.

The Freundlich isotherm helps to predict the monolayer or multilayer sorption configuration of sorbent after interaction with sorbate. Its linear form is given as follows:

$$\log q_e = \log k_F + \frac{1}{n}\log C_e \tag{9}$$

where the parameters q_e (mg g^{-1}) and C_e (mg L^{-1}) are the amounts of metal ions sorbed by the sorbent and the amounts of metal ions in liquid phase, k_F (sorption capacity) and n (sorption strength) are the Freundlich constants. A graph is plotted between $\log q_e$ and $\log C_e$ to fit isothermal experimental data into the Freundlich isotherm (Eq. (9)). Values of R^2, k_F, and n were obtained from the slope and intercept of the plot and tabulated (Table 1). The profound deviation of value of sorption capacity (Q_{max} in mg g^{-1}) calculated from Freundlich isotherm from experimental value (q_e in mg g^{-1}) and very low value of correlation coefficient (R^2) shows that this model is not suitable for present sorption study (Fig. 5a, Table 1). Therefore, the experimental data was further fitted into the Langmuir's isotherm to know about sorption mechanism. The linear form of Langmuir isotherm is given as:

$$\frac{C_e}{q_e} = \frac{C_e}{Q_{\max}} + \frac{1}{Q_{\max} \times b} \tag{10}$$

In Eq. (10), C_e is the equilibrium concentration of metal ions (mg L^{-1}) in liquid phase, q_e (mg g^{-1}) is the amount of metal ions uptake by sorbent, $Q_{\max}$ (mg g^{-1}) is the maximum sorption capacity per gram of sorbent, and b is constant associated with Langmuir's isotherm. A plot of graph between values of C_e/q_e and C_e, gives straight lines with high value of R^2 (0.99>) for both Cd^{2+} and Pb^{2+}. These straight lines suggested that the Langmuir model is found to be best fitted to the sorption data (Fig. 5b). The values of $Q_{\max}$ and Langmuir's constant b were determined from the slope and intercept of straight lines, respectively. The values of $Q_{\max}$ (303.03 for Cd^{2+} and 316.8 for Pb^{2+}) determined from this model were found to be quite compatible with experimental ones, that is, q_e (260.0 for Cd^{2+} and 293.33 for Pb^{2+}). Therefore, Langmuir's isothermal model is found to ideally fit to this sorption data and indicated that sorption of Cd^{2+} and Pb^{2+} followed chemisorption by forming a monolayer.

Table 1
Experimental sorption capacities, Langmuir, Freundlich, pseudo-second-order, pseudo-first-order, ion-exchange models, and thermodynamic parameters for Cd^{2+} and Pb^{2+} uptake by Na-SRG

Models	Parameters	Cd^{2+}	Pb^{2+}
Experimental	q_e (mg g^{-1})	260.0	293.33
Langmuir parameters	$Q_{\max}$ (mg g^{-1})	303.03	316.79
	b (mg L^{-1})	0.0569	0.08395
	R_L	0.1498	0.1064
	R^2	0.9990	0.9361
Freundlich parameters	n	1.3515	1.6425
	k_F	7.1681	15.1493
	R^2	0.9333	0.8989
Pseudo-second-order	q_e (mg g^{-1})	305.6	314.5
	k_2 (g mg^{-1} min^{-1})	0.0003	0.0006
	R^2	0.9938	0.9962
Pseudo-first-order	q_e (mg g^{-1})	163.04	75.32
	k_1 (g mg^{-1} min^{-1})	0.0368	0.0196
	R^2	0.9247	0.5411
Ion-exchange model	S (min^{-1})	0.047	0.0491
	R^2	0.9842	0.9782
Thermodynamic parameters	$\Delta S°$ (J mol^{-1} K^{-1})	–2.565	–1.333
	$\Delta H°$ (kJ mol^{-1})	–4.499	–5.295
	$\Delta G°$ (kJ mol^{-1})	–3.778	–4.844
	R^2	0.9672	0.9678

Moreover, among the essential features of this isotherm, a dimensionless constant, that is, separation factor (R_L) is also important one. Its value for both of the tested metals can be calculated using the following relation:

$$R_L = \frac{1}{1 + bC_i} \tag{11}$$

where C_i is the initial concentration of metal ions in mg L^{-1} and b is the Langmuir's equilibrium constant and calculated in L mg^{-1}. If value of R_L is 0, then sorption process is reversible, sorption is favorable if the value of R_L value is less than 1 but greater than 0, sorption is linear if R_L value is equal to 1, and sorption phenomenon is unfavorable if the value of R_L is greater than 1. As its value lies in between 0 and 1, that is, R_L (0.1498 for Cd^{2+} and 0.1064 for Pb^{2+}), therefore, it advises favorable sorption of both Cd^{2+} and Pb^{2+}, respectively. The validity of Langmuir model to the sorption data of present investigation also gave evince of the involvement of chemisorption by forming a monolayer (Fig. 5b, Table 1).

3.6. Kinetic modeling

The data obtained from contact time experiments were fitted into pseudo-first- and pseudo-second-order kinetic

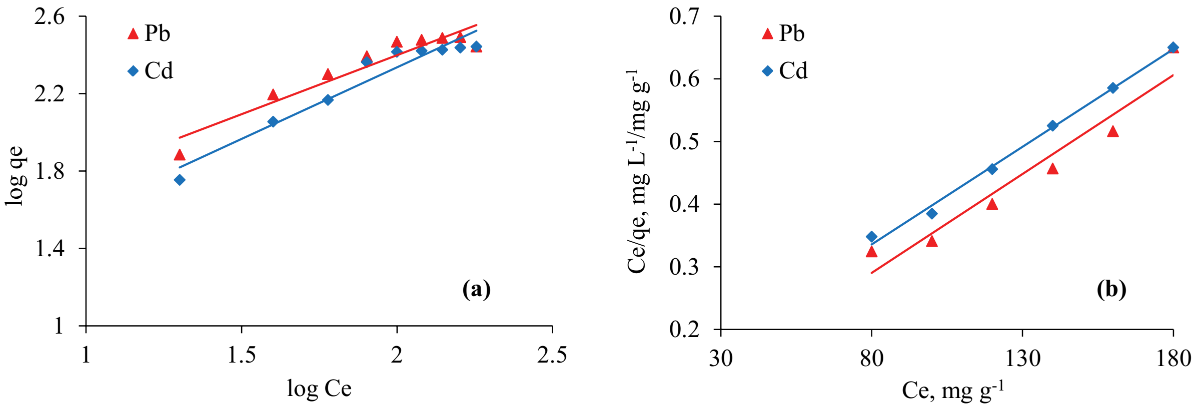

Fig. 5. Freundlich isotherm model (a), and Langmuir isotherm model (b) for Cd^{2+} and Pb^{2+} uptake from aqueous solution by Na-SRG sorbent.

models in order to establish the mechanism of Cd^{2+} and Pb^{2+} sorption, that is, either sorption is physio-sorption or chemisorption by Na-SRG. Eq. (12) embodies the linear form of pseudo-first-order kinetic model:

$$\log\left(q_e - q_t\right) = \log q_e - \frac{k_1}{2.303}t \tag{12}$$

where q_e (mg g^{-1}) and q_t (mg g^{-1}) represents the amount of metal sorbed on the sorbent surface at equilibrium and time t, respectively while k is velocity constant which is measured in (g mg^{-1} min^{-1}). The applicability of pseudo-first-order kinetic model to the sorption data was predicted by plotting a graph between the values of log(q_e – q_t) along the dependent axis (Y-axis) and time t along the independent axis (X-axis). The resulted graph has a low value of R^2 for both Cd^{2+} and Pb^{2+} and a big gap was also found between experimentally determined Cd^{2+} and Pb^{2+} sorption capacities of Na-SRG and as-calculated from the slope of straight line obtained after fitting data into pseudo-first-order kinetic model. So, this model couldn't give fruitful information to decide about the mechanism of sorption for tested metals by Na-SRG (Fig. 6a, Table 1). The data was further applied to pseudo-second-order kinetic model for said judgment. Eq. (13) can explain the mathematical configuration of this kinetic model.

$$\frac{t}{q_t} = \left(\frac{1}{kq_e^2} + \frac{t}{q_e}\right) \tag{13}$$

In Eq. (13), the factors q_e (mg g^{-1}) and q_t (mg g^{-1}) signifies the amount of metal ions sorbed on the surface of sorbent at equilibrium and time t (min), respectively while k (g mg^{-1} min^{-1}) is rate constant. Plot of the values of t/q_t against t give linearity in lines with slope and intercept. The slope of the linear plots gives the value of q_e (mg g^{-1}) and intercept agrees to the value of rate constant k (Table 1). High value of R^2 (0.99>) and compatibility of the experimental and theoretically calculated value of q_e in mg g^{-1} for both Cd^{2+} and Pb^{2+} was found. Therefore, said queries indicated the validity of pseudo-second-order kinetic model to the sorption data, and also it can be predicted that the removal of Cd^{2+} and Pb^{2+} from aqueous solution follows chemisorption (Fig. 6b, Table 1).

3.7. Ion-exchange model

Mechanism of sorption was determined to plaid the promising behavior of both SRG and Na-SRG during the sorption of Cd^{2+} and Pb^{2+}. SRG bared negligible sorption from both Cd^{2+} and Pb^{2+}, whereas, Na-SRG showed rationally high uptake. This might happen only because of the exchange of Cd^{2+} and Pb^{2+} ions of sorbate with Na^{1+} ions of sorbent, which is only possible in between solutions containing Cd^{2+} and Pb^{2+} and Na-SRG but no such exchange takes place in between solutions containing Cd^{2+} and Pb^{2+} and SRG (Fig. 7a). Boyd [38] derived an equation to explain the ion-exchange mechanism (Eq. (14)):

$$\log\left(1 - F\right) = -\frac{S}{2.303}t \tag{14}$$

$$F = \frac{q_t}{q_e} \tag{15}$$

where, q_e (mg g^{-1}) and q_t (mg g^{-1} min^{-1}) are the amounts of metal ions sorbed at equilibrium and time t, respectively, and S (min^{-1}) is a constant for sorption. Values of log(1 – F) were plotted against t to predict the involvement of ion-exchange mechanism. A straight line was obtained with a high value of R^2 for both Cd^{2+} and Pb^{2+}, which further substantiated the engrossment of ion-exchange mechanism during sorption of Cd^{2+} and Pb^{2+} from aqueous solution (Fig. 7a, Table 1).

3.8. Determination of thermodynamic parameters

In order to check the spontaneity of reaction, different thermodynamic parameters such as ΔG°, ΔS°, and ΔH° was calculated using sorption data obtained from the effect of temperature. The plot of graph between the values of lnK_C and 1/T (K^{-1}) gives straight lines with slope and intercepts

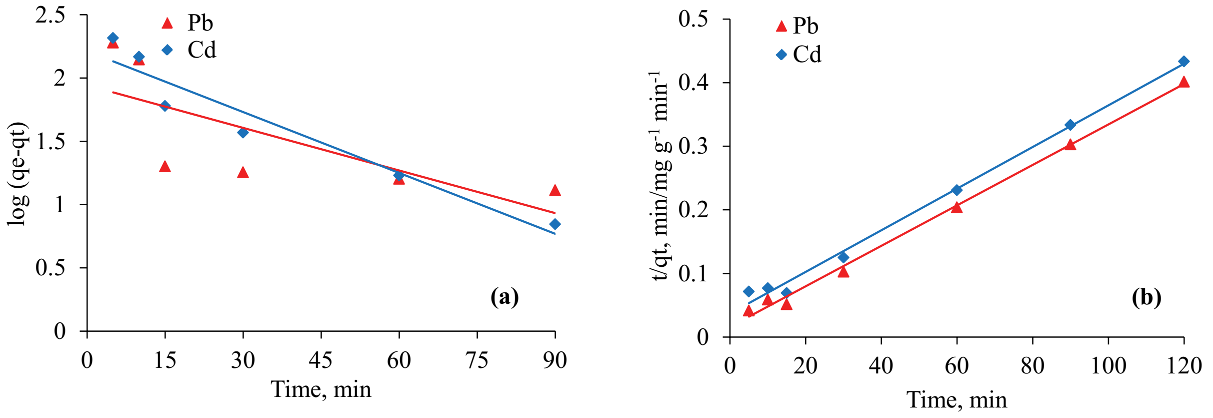

Fig. 6. Pseudo-first-order kinetic model (a), and pseudo-second-order kinetic model (b) for Cd^{2+} and Pb^{2+} uptake from aqueous solution by Na-SRG sorbent.

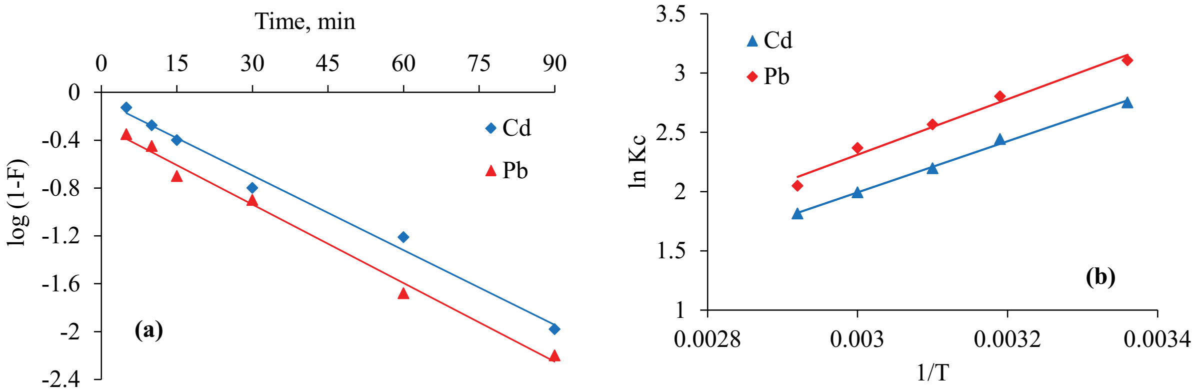

Fig. 7. Ion-exchange model (a), and effect of temperature on equilibrium constant (b) for Cd^{2+} and Pb^{2+} ions sorption by Na-SRG.

for metals under studies (Eq. (17)). Value of $\Delta H°$ can be calculated from the slope of graph and $\Delta S°$ from the intercept while the value of $\Delta G°$ was calculated using Eq. (18):

$$K_C = \frac{C_{\text{ads}}}{C_e} \tag{16}$$

where C_{ads} represents the value of amount of metal sorbed in mg g^{-1}, C_e shows the equilibrium concentration of metal in mg g^{-1} and K_C is the equilibrium constant:

$$\ln K_C = \frac{\Delta S°}{R} - \frac{\Delta H°}{RT} \tag{17}$$

$$\Delta G° = -RT \times \ln K_C \tag{18}$$

In Eqs. (16) and (17), R is the ideal gas constant, T is the absolute temperature measured in Kelvin, and K_C (L mol^{-1}) is the equilibrium constant. Negative values of $\Delta H°$ and $\Delta G°$ were obtained which indicated the feasibility, spontaneity, and exothermic nature of the sorption process, whereas the negative value of $\Delta S°$ indicates decrease in the degree of freedom for sorbed Cd^{2+} and Pb^{2+} due to the presence of strong sorbent–sorbate interaction during the process of sorption (Table 1).

3.9. Sorption–desorption (regenerability)

Experiments regarding the regenerability of spent Na-SRG were also carried out under optimum conditions. Results of sorption–desorption studies of Cd^{2+} and Pb^{2+} are presented in Figs. 8a and b. A decrease in sorption capacity for Cd^{2+} and Pb^{2+} was found to be 32 and 28 mg g^{-1}, respectively after five cycles. Figs. 8a and b show the net decrease in percentage sorption and it was found to be 7% for Cd^{2+} and 8% for Pb^{2+} after five repetitive cycles. Therefore, these results suggested that the given sorbent can be re-used before need to replace.

The position of the present sorbent (Na-SRG) was also compared with already reported modified sorbents for uptake of Cd^{2+} and Pb^{2+} from an aqueous solution (Table 2). It was found that Na-SRG had a distinct position among the other polysaccharide-based sorbents for Cd^{2+} and Pb^{2+} removal.

The values of sorption capacities (Q_{max} in mg g^{-1}) presented in Table 2 were calculated by Langmuir isothermal model.

Table 2
Comparison of Na-SRG sorption capacity with some other polysaccharide-based modified reported sorbents for Cd^{2+} and Pb^{2+} sorption

Biosorbent	Target metal ion	Sorption capacity (mg g^{-1})	References
Cellulosic okra fibers (acrylonitrile/methacrylic acid)	Pb^{2+}	268.32	[39]
Mercerized cellulose and sugarcane bagasse (modified with EDTA dianhydride)	Cd^{2+} and Pb^{2+}	87.7–149 and 192–333	[40]
Cellulose (modified with succinic anhydride)	Cd^{2+}	185.2 DW and 178.6 GW	[41]
Agriculture waste biomass (modified with succinic anhydride)	Cd^{2+} and Pb^{2+}	121.57 and 273.97	[42]
Wood (modified with citric acid)	Pb^{2+}	82.64	[43]
Sugar can bagasse (modified with citric acid and Fe_3O_4)	Cd^{2+} and Pb^{2+}	33.2 and 116.7	[44]
Spent grain (modified with sodium hydroxide)	Cd^{2+} and Pb^{2+}	17.3 and 35.5	[45]
Poly(vinyl alcohol)/chitosan	Pb^{2+}	166	[46]
Rhamnogalacturonans (modified with succinic anhydride)	Cd^{2+} and Pb^{2+}	303.03 and 316.79	Present study

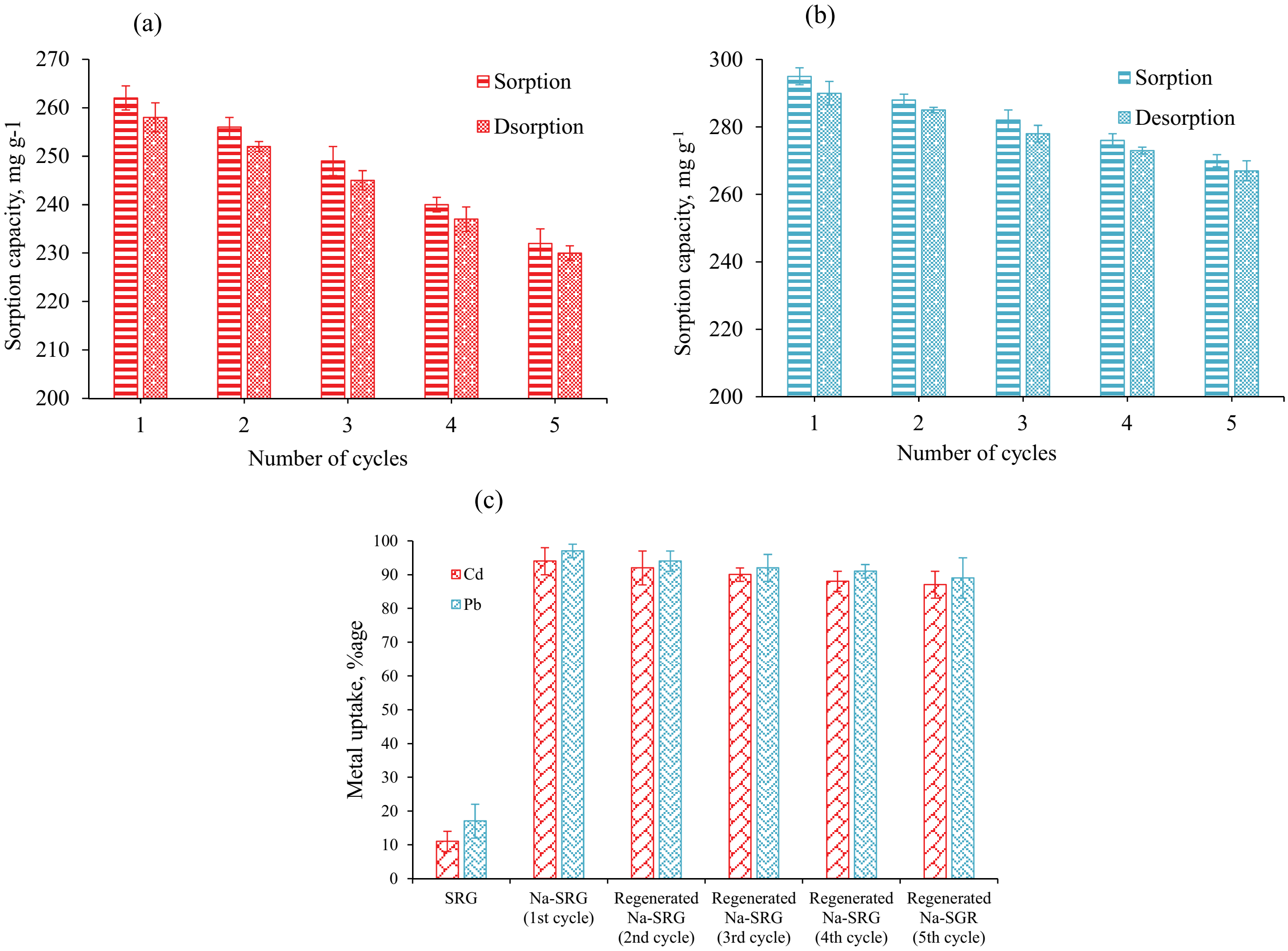

Fig. 8. Sorption and desorption values for Cd^{2+} (a), Pb^{2+} ions (b), and percentage metal-uptake by the acidic (SRG) and sodic form of sorbent (Na-SRG) over five cycles by Na-SRG from aqueous solution (c).

4. Conclusions

Succinylated rhamnogalacturonans (SRG) and its sodium salt (Na-SRG) were successfully prepared *via* esterification. The sorbent (Na-SGR) was found to be strongly dependent on operational parameters. The order of sorption was $Cd^{2+} < Pb^{2+}$. Moreover, it was determined that more than 85% of both Cd^{2+} and Pb^{2+} uptakes reached within 30 min, which revealed that sorption followed the ion-exchange via chemisorption. The negative values of different thermodynamic parameters and insignificant decrease in sorption capacities after five repetitive cycles, confirmed the performance of sorption mechanism is spontaneous and exothermic and Na-SRG is a re-generable and reusable sorbent. Notably, the high sorption capacity and the kinetic results showed that Na-SRG can be used as the selective sorbent for removal of Cd^{2+} and Pb^{2+} from aqueous solution. Consequently, it can also be established that Na-SRG is a very efficient and reusable supersorbent for Cd^{2+} and Pb^{2+} uptake from aqueous solution.

Acknowledgments

MH is grateful to ORIC University of Sargodha Pakistan for the financial support under grant number UOS/ORIC/2016/52 for the project “Removal of heavy metal ions from aqueous solution using chemically modified polysaccharide.”

References

[1] N. Karakaya, M.C. Karakaya, Toxic element contamination in waters from the massive sulfide deposits and wastes around Giresun, Turkey, Turk. J. Earth Sci., 23 (2014) 113–128.
[2] P. Kurzweil, W. Scheuerpflug, State-of-charge monitoring and battery diagnosis of NiCd cells using impedance spectroscopy, Batteries, 6 (2020), doi: 10.3390/batteries6010004.
[3] H. Liu, K. Liu, H. Fu, R. Ji, X. Qu, Sunlight mediated cadmium release from colored microplastics containing cadmium pigment in aqueous phase, Environ. Pollut., 263 (2020), doi: 10.1016/j.envpol.2020.114484.
[4] A. Turner, Cadmium pigments in consumer products and their health risks, Sci. Total Environ., 657 (2019) 1409–1418.
[5] P. Vanysek, P. Baca, J. Zimakova, S. Vaculik, M. Bouska, *In-situ* AFM observations of the effect of addition of glass fibers and

lignosulfonates on performance of the negative active mass of a lead-acid storage battery, J. Energy Storage, 29 (2020), doi: 10.1016/j.est.2020.101318.

[6] E. Hernandez, J. Obrist-Farner, M. Brenner, W.F. Kenney, J.H. Curtis, E. Duarte, Natural and anthropogenic sources of lead, zinc, and nickel in sediments of Lake Izabal, Guatemala, J. Environ. Sci., 96 (2020) 117–126.

[7] Ihsanullah, F.A. Al-Khaldi, B. Abusharkh, M. Khaled, M.A. Atieh, M.S. Nasser, T. Laoui, T.A. Saleh, S. Agarwal, I. Tyagi, V.K. Gupta, Adsorptive removal of cadmium(II) ions from liquid phase using acid modified carbon-based adsorbents, J. Mol. Liq., 204 (2015) 255–263.

[8] P.S. Kumar, K. Kirthika, K.S. Kumar, Removal of hexavalent chromium ions from aqueous solutions by an anion-exchange resin, Adsorpt. Sci. Technol., 26 (2008) 693–703.

[9] Z. Shan, Z. Wei, Z.A. Shaikh, Suppression of ferroportin expression by cadmium stimulates proliferation, EMT, and migration in triple-negative breast cancer cells, Toxicol. Appl. Pharmacol., 356 (2018) 36–43.

[10] A. Buha, D. Wallace, V. Matovic, A. Schweitzer, B. Oluic, D. Micic, V. Djordjevic, Cadmium exposure as a putative risk factor for the development of pancreatic cancer: three different lines of evidence, Biomed. Res. Int., 2017 (2017) 1–8.

[11] C.Y. Lee, C.H. Su, P.K. Tsai, M.L. Yang, Y.C. Ho, S.S. Lee, C.H. Chen, W.Y. Chen, M.L. Lin, C.J. Chen, C.Y. Chian, R.H. Liu, Y.L. Chang, Y.H. Kuan, Cadmium nitrate-induced neuronal apoptosis is protected by N-acetyl-l-cysteine via reducing reactive oxygen species generation and mitochondria dysfunction, Biomed. Pharmacother., 108 (2018) 448–456.

[12] H. Al-Mahbashi, S. Asfoura, S. Obri, T. Al-Maqtari, A. Abudunia, Level of lead in the blood among fuel station employees and its relationship to impaired liver and kidney functions in damascus; syria: occupational exposure to lead, Univ. J. Pharm. Res., 5 (2020) 10–15.

[13] M. Naushad, Surfactant assisted nano-composite cation exchanger: development, characterization and applications for the removal of toxic Pb^{2+} from aqueous medium, Chem. Eng. J., 235 (2014) 100–108.

[14] J. Tang, J. Xi, J. Yu, R. Chi, J. Chen, Novel combined method of biosorption and chemical precipitation for recovery of Pb^{2+} from wastewater, Environ. Sci. Pollut. Res., 25 (2018) 28705–28712.

[15] J. Kheriji, D. Tabassi, B. Hamrouni, Removal of Cd(II) ions from aqueous solution and industrial effluent using reverse osmosis and nanofiltration membranes, Water Sci. Technol., 72 (2015) 1206–1216.

[16] Y.H. Kotp, Enhancement of industrial effluents quality by using nanocomposite Mg/Al LDH ultrafiltration membranes, J. Inorg. Organomet. Polym. Mater., 30 (2020) 5244–5260.

[17] T.K. Tran, K.F. Chiu, C.Y. Lin, H.J. Leu, Electrochemical treatment of wastewater: selectivity of the heavy metals removal process, Int. J. Hydrogen Energy, 42 (2017) 27741–27748.

[18] G. Sharma, M. Naushad, Adsorptive removal of noxious cadmium ions from aqueous medium using activated carbon/zirconium oxide composite: isotherm and kinetic modeling, J. Mol. Liq., 310 (2020), doi: 10.1016/j.molliq.2020.113025.

[19] W. Zuo, C. Chen, H. Cui, M. Fu, Enhanced removal of Cd(II) from aqueous solution using $CaCO_3$ nanoparticle modified sewage sludge biochar, RSC Adv., 7 (2017) 16238–16243.

[20] M.A. Hussain, D. Shawar, M.N. Hassan, M.N. Tahir, M.S. Iqbal, M. Sher, An efficient esterification of pullulan using carboxylic acid anhydrides activated with iodine, Collect. Czech. Chem. Commun., 75 (2010) 133–143.

[21] M.A. Hussain, K. Abbas, I. Jantan, S.N.A. Bukhari, Polysaccharide-based materials in macromolecular prodrug design and development, Int. Mater. Rev., 62 (2016) 78–98.

[22] M.T. Haseeb, M.A. Hussain, S.H. Yuk, S. Bashir, M. Nauman, Polysaccharides based superabsorbent hydrogel from linseed: dynamic swelling, stimuli responsive on-off switching and drug release, Carbohydr. Polym., 136 (2016) 750–756.

[23] F.A. Sheikh, M.A. Hussain, M.U. Ashraf, M.T. Haseeb, M. Farid-ul-Haq, Linseed hydrogel based floating drug delivery system for fluoroquinolone: design, *in vitro* drug release and *in vivo* real-time floating detection, Saudi Pharm. J., 28 (2020) 538–549.

[24] M.T. Haseeb, M.A. Hussain, S. Bashir, M.U. Ashraf, N. Ahmad, Evaluation of superabsorbent linseed-polysaccharides as a novel stimuli-responsive oral sustained release drug delivery system, Drug Dev. Ind. Pharm., 43 (2017) 409–420.

[25] A. Abbas, M.A. Hussain, M. Amin, M. Sher, M.N. Tahir, W. Tremel, Succinate-bonded pullulan: an efficient and reusable super-sorbent for cadmium-uptake from spiked high-hardness groundwater, J. Environ. Sci., 37 (2015) 51–58.

[26] B.A. Lodhi, A. Abbas, M.A. Hussain, S.Z. Hussain, M. Sher, I. Hussain, Design, characterization and appraisal of chemically modified polysaccharide based mucilage from *Ocimum basilicum* (basil) seeds for the removal of Cd(II) from spiked high-hardness ground water, J. Mol. Liq., 274 (2019) 15–24.

[27] M.A. Hussain, G. Muhammad, I. Jantan, S.N.A. Bukhari, Psyllium arabinoxylan: a versatile biomaterial for potential medicinal and pharmaceutical applications, Polym. Rev., 56 (2016) 1–30.

[28] G. Muhammad, A. Abbas, M.A. Hussain, M. Sher, S.N. Abbas, Chemically modified glucuronoxylan: a novel material for heavy metal ion removal from aqueous and spiked high hardness groundwater, Cellul. Chem. Technol., 52 (2018) 909–919.

[29] A. Abbas, M.A. Hussain, M. Sher, S.Z. Hussain, I. Hussain, Evaluation of chemically modified polysaccharide pullulan as an efficient and regenerable supersorbent for heavy metal ions uptake from single and multiple metal ion systems, Desal. Water Treat., 78 (2017) 241–252.

[30] A. Abbas, M.A. Hussain, M. Sher, M.I. Irfan, M.N. Tahir, W. Tremel, S.Z. Hussain, I. Hussain, Design, characterization and evaluation of hydroxyethylcellulosebased novel regenerable supersorbent for heavy metal ions uptake and competitive adsorption, Int. J. Biol. Macromol., 102 (2017) 170–180.

[31] W. Stumm, H. Hohl, F. Dalang, Interaction of metal ions with hydrous oxide surfaces, Croat. Chem. Acta, 48 (1976) 491–504.

[32] Y. Jiao, D. Han, Y. Lu, Y. Rong, L. Fang, Y. Liu, R. Han, Characterization of pine-sawdust pyrolytic char activated by phosphoric acid through microwave irradiation and adsorption property toward CDNB in batch mode, Desal. Water Treat., 77 (2017) 247–255.

[33] L. Zhang, W. Li, H. Cao, D. Hu, X. Chen, Y. Guan, J. Tang, H. Gao, Ultra-efficient sorption of Cu^{2+} and Pb^{2+} ions by light biochar derived from *Medulla tetrapanacis*, Bioresour. Technol., 291 (2019), doi: 10.1016/j.biortech.2019.121818

[34] X. Jiang, H. Ruib, G. Chena, B. Xing, Facile synthesis of multifunctional bone biochar composites decorated with Fe/Mn oxide micro-nanoparticles: physicochemical properties, heavy metals sorption behavior and mechanism, J. Hazard. Mater., 399 (2020), doi: 10.1016/j.jhazmat.2020.123067.

[35] Y.H. Kotp, M.E.A. Ali, S.A. Mohallal, M.M.S. Aboelfadl, Synthesis of a novel inorganic cation exchanger based on molybdate: applications for removal of Pb^{2+}, Fe^{3+} and Mn^{2+} ions from polluted water, Sep. Sci. Technol., 54 (2018) 620–633.

[36] Y.H. Kotp, Controlled synthesis and sorption properties of magnesium silicate nanoflower prepared by a surfactant-mediated method, Sep. Sci. Technol., 52 (2017) 657–670.

[37] E.R. Soliman, Y.H. Kotp, E.R. Souaya, K.A. Guindy, R.G.M. Ibrahim, Development the sorption behavior of nanocomposite Mg/Al LDH by chelating with different monomers, Composites, Part B, 175 (2019), doi: 10.1016/j.compositesb.2019.107131.

[38] G.E. Boyd, A.W. Adamson, L.S. Myers, The exchange adsorption of ions from aqueous solutions by organic zeolites. II. Kinetics, J. Am. Chem. Soc., 69 (1947) 2836–2848.

[39] A.S. Singha, A. Guleria, Chemical modification of cellulosic biopolymer and its use in removal of heavy metal ions from wastewater, Int. J. Biol. Macromol., 67 (2014) 409–417.

[40] O. Karnitz Jr., L.V.A. Gurgel, R.P. de Freitas, L.F. Gil, Adsorption of Cu(II), Cd(II), and Pb(II) from aqueous single metal solutions by mercerized cellulose and mercerized sugarcane bagasse chemically modified with EDTA dianhydride (EDTAD), Bioresour. Technol., 77 (2009) 643–650.

[41] B. Belhalfaoui, A. Aziz, E.H. Elandaloussi, M.S. Ouali, L.C. De-Menorval, Succinate-bonded cellulose: a regenerable

and powerful sorbent for cadmium removal from spiked high-hardness groundwater, J. Hazard. Mater., 169 (2009) 831–837.

[42] A.S. Singha, A. Guleria, Utility of chemically modified agricultural waste okra biomass for removal of toxic heavy metal ions from aqueous solution, Eng. Agric. Environ. Food, 8 (2015) 52–60.

[43] K.S. Low, C.K. Lee, S.M. Mak, Sorption of copper and lead by citric acid modified wood, Wood Sci. Technol., 38 (2004) 629–640.

[44] G. Liu, L. Liao, Z. Dai, Q. Qi, J. Wu, L.Q. Ma, C. Tang, J. Xua, Organic adsorbents modified with citric acid and Fe_3O_4 enhance the removal of Cd and Pb in contaminated solutions, Chem. Eng. J., 95 (2020), doi: 10.1016/j.cej.2020.125108.

[45] K.S. Low, C.K. Lee, S.C. Liew, Sorption of cadmium and lead from aqueous solutions by spent grain, Process Biochem., 36 (2000) 59–64.

[46] X. Li, Y. Li, Z. Ye, Preparation of macroporous bead adsorbents based on poly(vinyl alcohol)/chitosan and their adsorption properties for heavy metals from aqueous solution, Chem. Eng. J., 178 (2011) 60–68.